THE ASTROPHYSICAL JOURNAL, 347:1090–1099, 1989 December 15

SHOCK-GENERATED X-RAY EMISSION IN RADIATIVELY DRIVEN WINDS: A MODEL FOR TAU SCORPII

JOSEPH J. MACFARLANE
Fusion Technology Institute, University of Wisconsin, Madison, WI 53706

AND

JOSEPH P. CASSINELLI
Department of Astronomy, University of Wisconsin, Madison, WI 53706
Received 1989 March 2; accepted 1989 June 17

ABSTRACT

We use a one-dimensional radiation-hydrodynamics code to numerically investigate the structure and evolution of shocks in the winds of hot stars. Results are presented for the specific case of τ Sco, a well-studied main-sequence B star for which there are X-ray data from the *Einstein* satellite's Solid State Spectrometer. Using a phenomenological radiative acceleration term and a mass-loss rate consistent with UV observations, we determine the time-dependence of the temperatures within and X-ray emission from an isolated shock region. The driving acceleration leads to the formation of a two-component shock zone with "forward" and "reverse" shocks, each with their own characteristic temperature. A denser cold region forms between the two shocks, which could potentially account for the presence of narrow absorption features that are observed in the UV P Cygni profiles of many hot stars. We find the X-ray emission spectra from the shocks in our calculations are in good general agreement with two-temperature model fits to *Einstein* X-ray observations.

Subject headings: shock waves — stars: early-type — stars: individual (τ Sco) — stars: winds — stars: X-rays — X-rays: spectra

I. INTRODUCTION

The X-ray emission from early-type stars provides the best information concerning the presence of high-speed wind shocks or coronal zones in their outer atmospheres. O and early B stars typically have X-ray luminosities of about 10^{-7} times their total stellar luminosity. Fitting the X-ray spectra obtained with the Solid State Spectrometer (SSS) aboard the *Einstein* satellite—which provides the highest spectral resolution to date—often requires a two-component source structure. Both the OB supergiants and the OB main-sequence stars typically have a low-temperature component with $T \sim 3$–8×10^6 K and a high-temperature component with $T > 10^7$ K (Cassinelli and Swank 1983; Swank 1985). Other evidence for the presence of hot gas in the outer atmosphere is provided by UV observations of P Cygni profiles of highly charged ("superionized") ions (Lamers and Morton 1976; Lamers and Rogerson 1978; Olson and Castor 1981). Superionization of the relatively cool part of the wind can be caused by either Auger ionization that naturally results from the X-ray emission of the stars (Cassinelli and Olson 1979), or by collisional ionization in warm winds (Lamers and Morton 1976; Hamann 1981). For early O stars, the ions can be produced collisionally in regions of the wind where the He II continuum is optically thick (Pauldroch 1987). It is generally accepted that the high speeds of the winds of early-type stars are explained by the line radiation force theory of Castor, Abbott, and Klein (1975, hereafter CAK). However, CAK theory does not explain the presence of high-temperature material or the widely observed time variability of the spectral lines that are formed in the wind. The UV P Cygni profiles often have narrow absorption features superposed on them (Lamers, Gathier, and Snow 1982; Henrichs 1988; Prinja and Howarth 1986), suggesting that the winds do not have smooth velocity and density distributions as predicted by CAK theory, but rather have some "clumping" associated with them. In some cases the density concentrations appear to originate deep in the wind and advect outward with the wind (Gry, Lamers, and Vidal-Madjar 1984; Henrichs, Kaper, and Zwarthoed 1988). Although the primary purpose in this paper is to explain the X-ray properties of one well-observed star, τ Sco, we shall find that shock models also provide useful insight into the variability, superionization, and clumpiness associated with hot star winds.

There have been two types of models proposed to explain the X-ray emission of early type stars: a model in which the X-rays originate in a hot corona at the base of a much cooler wind, and a model in which there are hot zones embedded in the wind in the form of shocks which can arise from instabilities in the line-driven winds. Cassinelli and Olson (1979) proposed the base corona plus cool wind model to explain the presence of strong resonance lines of superionization stages such as O VI 1040 Å and N V 1250 Å in *Copernicus* satellite observations. Their model predicted rather well the X-ray luminosities of Of stars, but it did not predict the observed X-ray spectral energy distribution. The overlying cool wind was predicted to produce more attenuation of the X-rays between 0.6 and 1.0 keV than was seen in the *Einstein* spectra (Long and White 1980; Cassinelli *et al.* 1981; Cassinelli and Swank 1983). Waldron (1984) has argued, however, that this difficulty with coronal models can partly be overcome by accounting for changes in the ionization balance above the coronal zone, and finds that coronal models cannot be ruled out.

Embedded shock models overcome the attenuation problem because the source of the X-rays is farther out in the wind, above much of the absorbing matter. In the models of Lucy and White (1980) and Lucy (1982), shocks are formed as radiatively driven regions overtake "shadowed", i.e., non-radiatively driven, gas ahead of them. The model of Lucy,

however, predicts shock-produced X-ray luminosities that are a factor of 20 too low, and characteristic X-ray temperatures $\lesssim 10^6$ K (Lucy 1982). Thus, shock models also appear to be incomplete and have not yet led to a fully satisfactory picture for understanding the observations of stellar X-rays.

Nevertheless, there has been a great deal of recent progress in the general understanding of shocks in the winds of hot stars. Krolik and Raymond (1985) examined the structure and emission rates of time-steady shocks. Owocki and Rybicki (1984) and Rybicki, Owocki, and Castor (1988) have studied the stability of radiatively driven flows. Owocki, Castor, and Rybicki (1988, hereafter OCR) studied the growth of radiatively driven instabilities in isothermal flows driven by pure absorption and found that strong shocks form with velocity jumps $\sim$500–1000 km s^{-1}. In addition to the potential to produce better agreement with X-ray spectral observations, shock models can also account for the narrow absorption features observed in the P Cygni profiles of many O and B stars (Lamers *et al.* 1982; Mullan 1984).

In this paper we will focus primarily on the B0 main sequence star τ Sco. It is one of only six hot stars that was observed using the relatively high resolution Solid State Spectrometer. The data indicate that, as for OB supergiants, a two-component model is required to fit the observed spectral energy distribution (Swank 1985). The star also has a well-studied UV spectrum. By analyzing the UV resonance lines observed with *Copernicus* satellite, Lamers and Rogerson (1978, hereafter LR) have been able to derive constraints on the velocity and density distribution of the wind. One of their most puzzling results is that the relative populations of superionization states N v and O vi decrease in the outward direction near the base of the wind. This is in contrast to what is expected from models in which the superionization is explained by a radiative process, such as Auger ionization due to X-rays originating in either a corona or an external hot shock region. This could be explained by a warm wind model in which there is a temperature decrease in the outward direction (Hamann 1981), but it is unclear what mechanism would be responsible for maintaining the warm temperatures.

The purpose of this paper is to determine whether the observed X-ray emission from τ Sco can be explained by a shock model in which the wind density and velocity are consistent with UV observations. We also discuss the observational consequences of our model. We use a one-dimensional Lagrangian radiation-hydrodynamics code to study the temperature and X-ray emission rate of an isolated shock region moving through a model wind for τ Sco. Observational data are used to constrain the bulk properties and radiative acceleration of the wind. Our basic approach of the problem is as follows. From the SSS data we have information concerning the temperatures of the X-ray emitting regions. These temperatures immediately lead to information concerning the velocity jumps that must exist across at least some of the shock fronts in the wind. We set up plausible conditions that allow such shock strengths to occur and numerically compute the time-dependent structure of individual shock regions propagating through the wind. It is assumed that the wind is driven by line forces. However, in this paper we choose not to use a detailed description of the driving such as that in the CAK model for hot star winds. We use a simpler radiative force model in which the radiative acceleration is a simple function of the wind temperature so that the force in the high-temperature, highly ionized shock region is small. The mass-loss rate and terminal velocity in our model are chosen to be within the general limits defined by UV observations.

We find that the driving acceleration in our model leads to an interesting "driven wave" type of shock structure that has been discussed in regards to the solar wind (Hundhausen and Gentry 1969; Hundhausen 1985). This is a two-component shock structure in which there is an outward facing shock occurring where a shock region overtakes the material in front of it, and there is a starward facing shock that is caused by the radiative driving of material into the shock. OCR recently found that forward and reverse shocks can arise from instabilities in radiatively driven winds, with the reverse shock being significantly stronger than the forward shock. However, because their calculation assumed an isothermal wind—i.e., the energy equation is not solved—the temperatures and X-ray emission of the shock regions could not be determined. Thus, our calculation is in many respects complimentary to theirs. After calculating the time-dependent temperature distribution within a shock region moving through a model wind for τ Sco, we compute the X-ray spectra at several times and compare with observational data.

In § II, we review the observational constraints for the wind of τ Sco provided by UV and X-ray observations. Details of our numerical calculations are described in § III. In § IV, we present results for the structure and evolution of the shock region, focusing especially on the temperatures in the shock region and the X-ray emission. We also discuss the consistency between our results and observations. Finally, we summarize our results in § V.

II. OBSERVATIONAL CONSTRAINTS FOR TAU SCORPII

a) UV Observations

Tau Sco has been extensively studied in the ultraviolet using the high resolution UV spectrometer aboard the *Copernicus* satellite (Rogerson and Upson 1977). Extended shortward absorption wings in several resonance lines—C III, C IV, N III, N V, O VI, Si IV, and P V—indicate the presence of a moderate density wind with a terminal velocity of at least 2000 km s^{-1} (LR). The lack of significant emission features in the P Cygni profiles may well signify that UV radiation scattered by the wind is occulted by the star, and that the absorption features are due to ions located rather close to the star. The mass loss rate was initially estimated by LR to be $0.7 \times 10^{-8}\ M_\odot$ yr^{-1}. Gathier, Lamers, and Snow (1981) substantially revised this estimate upward to $6.6 \times 10^{-8}\ M_\odot$ yr^{-1}. The major difficulty in determining the mass-loss rate arises from uncertainties in the ionization balance throughout the wind.

One notable feature that is absent from τ Sco's P Cygni profiles is any evidence of enhanced absorption within narrow velocity bands. These "narrow absorption features" have been detected in the P Cygni profile of many hot stars with strong winds (Lamers, Gathier, and Snow 1982; Henrichs 1988). Their absence is thought to be a result of τ Sco having a relatively small mass-loss rate and weak P Cygni profiles.

Another rather interesting determination made from UV observations of τ Sco is that the fractional abundances of superionization states N v and O vi tend to decrease as the wind velocity increases between 250 and 1000 km s^{-1} (LR; Morton 1979). This is significant because it may indicate that Auger ionization is not entirely responsible for populating the superionization states. In the steady-state Auger ionization model, the fractional abundances of superionization states are

proportional to the ratio of the Auger ionization rate to the radiative recombination rate (Cassinelli and Olson 1979). Thus, the fractional abundances of N V and O VI should vary as $q \propto J(r)/n_e \propto r^2 v J(r)$, where $J(r)$ is the mean intensity at a distance r from the center of the star, n_e is the electron density, and v is the wind velocity. This relation assumes the ionization fractions of N V and O VI are small, and that the mass flux throughout the wind is constant, $\dot{M} = 4\pi r^2 \rho v$. If the X-rays originate in shocks spaced throughout the wind, J varies little with r, and $q \propto r^2 v$. If the X-ray source is at the base of the wind and the density is low enough that absorption is unimportant, $J \propto r^{-2}$ and $q \propto v$. In either case, the ionization fractions of N V and O VI are predicted to increase with velocity, contrary to what is inferred from UV observations. According to LR, this disagreement suggests that the material at the base of τ Sco's wind is warm ($\sim 2 \times 10^5$ K), and the N V and O VI states are populated predominantly by collisions. It is not clear, however, what mechanism would be responsible for maintaining the wind at this temperature, since the wind should rapidly cool due to expansion.

b) *X-Ray Observations*

Observations of the X-ray emission from τ Sco using the Solid State Spectrometer aboard the *Einstein Observatory* have been reported by Swank (1985) and Cassinelli (1985, 1986). As is the case for many hot stars, a two-temperature model is needed to fit the observed spectrum adequately. For τ Sco, this consists of a low-temperature component with $T = 5.3 \times 10^6$ K and emission measure ($EM \equiv \int d^3 r n_e^2$) of 3×10^{54} cm^{-3}), and a high-temperature component with $T > 10^7$ K. For the high-temperature component the emission measure is poorly defined, but if $T \simeq 1.5 \times 10^7$ K the EM is constrained to be near $10^{53.5}$ cm^{-3} (Swank 1985). Two observations separated by one year using the low-resolution Imaging Proportional Counter (IPC) aboard the *Einstein* satellite showed no significant change in the overall X-ray flux (Waldron 1989). Recently, Collura *et al.* (1989) have carried out a variability analysis of OB stars. They found evidence for marginal variability ($\sim 3\ \sigma$ level) in τ Sco with an effective amplitude of roughly 30% over rather short time scales of about 50 s.

The wind column density of material above the X-ray source can be inferred from the photoabsorption by oxygen K shell electrons below 1 keV. Swank reports an upper limit of 2×10^{21} cm^{-2}. Using the velocity law suggested for τ Sco by LR, the column density of the wind above a point r' is

$$N_{\rm H} = \int_{r'}^{\infty} dr\, n_{\rm H} = C \int_{x'}^{\infty} \frac{dx}{x(x-1)} \qquad (1)$$

where

$$C = \frac{\dot{M} N_{\rm A}}{4\pi \mu R_* v_\infty},$$

$x \equiv r/R_*$, R_* is the stellar radius ($= 6.7\ R_\odot$), v_∞ is the terminal velocity ($= 2000$ km s^{-1}), $\dot{M}$ is the mass-loss rate, $N_{\rm A}$ is Avogadro's number, and μ is the mean atomic weight of the wind. Using the Gathier, Lamers, and Snow (1981) value of $\dot{M}$, $C = 2 \times 10^{21}$ cm^{-2}, which implies $r' \geq 1.6 R_*$ and $v(r') \geq 700$ km s^{-1}. This would suggest that the X-ray source may be embedded in the wind far above the photosphere. On the other hand, if we use the value of $\dot{M}$ determined by LR, we find $C = 2 \times 10^{20}$ cm^{-2} and $r'/R_* \simeq 1$. In this case, the overlying column density does not constrain the location of the X-ray source.

If the X-rays originate in strong shocks embedded in the wind, the temperatures deduced from the X-ray spectrum can be used to estimate the shock velocity and the relative fluid velocities at the shock front. Using the Rankine-Hugoniot relations (Zeldovich and Raizer 1966), which neglect energy loss and transport effects, the shock velocity relative to the ambient material ahead of the shock is

$$V_s = 1000 \text{ km s}^{-1} (T_s/1.3 \times 10^7 \text{ K})^{1/2}, \qquad (2)$$

where T_s is the temperature behind the shock. Thus, for τ Sco the shock velocities needed to reproduce the X-ray observations are 640 and 1100 km s^{-1} for the low- and high-temperature components, respectively. Similarly, the fluid velocity behind each shock front relative to the material ahead of it ($\Delta v_f = \frac{3}{4} V_s$) is 500 and 810 km s^{-1}. Although these estimated velocities represent a sizable fraction of the terminal velocity, they are consistent with narrow absorption features found for several O stars at 25%–50% below the terminal velocity (Lamers, Gathier, and Snow 1982).

III. OVERVIEW OF NUMERICAL CALCULATIONS

In this section, we describe the models and assumptions used in our time-dependent radiation-hydrodynamic calculations. In these calculations, shocks form as material near the base of the wind is accelerated to higher velocities than the material in front of it, thereby establishing a two-component velocity distribution. The scattering and absorption of photospheric radiation by bound-bound transitions is generally believed to be responsible for the rapid acceleration in stellar winds of hot stars. Below we describe calculations for shocks forming in a two-component wind that arise from a change in the radiative acceleration. We have chosen not to model the radiative acceleration in detail, but rather to set up initial conditions which allow a shock to form and study the structure and X-ray emission of the shock as it propagates through the wind. Our calculation is unlike that of OCR in that we have not attempted to study the formation mechanism of the shocks. Instead, we assume that shocks somehow form within the wind and examine the structure and evolution of the shock region. Although the detailed structure of the shocks in our calculations are somewhat different than that of OCR, many of the qualitative features are similar. Other than the formation mechanism, the primary difference between our calculation and that of OCR is that we solve both the momentum and energy equations—as opposed to only the momentum equation—so that we can examine the temperature structure within the shock, and study the effects of radiative cooling and thermal conduction on the shock structure. This allows us to calculate the X-ray spectrum and compare it with observational results.

To study the dynamics of shocks moving through stellar winds, we have performed numerical simulations using a one-dimensional, Lagrangian radiation-hydrodynamics code (Peterson, MacFarlane, and Moses 1988). Spherical symmetry is assumed. In the Lagrangian formulation, the conservation of mass and momentum equations are

$$\frac{dm_j}{dt} = 0, \qquad (3)$$

$$\frac{du}{dt} = \frac{1}{\rho}\frac{d}{dr}(P + Q) + g_{\rm rad} - g_*(R_*/r)^2, \qquad (4)$$

where m_j is the mass of the jth Lagrangian cell, t is the time, r is the radial position, u is the fluid velocity, ρ is the mass density, P is the gas pressure, Q is the artificial viscosity (see, e.g., Von Neumann and Richtmyer 1950), $g_{\rm rad}$ is the radiative acceleration, and g_* is the gravitational acceleration at the photosphere. We take g_* to be 1.4×10^4 cm s^{-1} (LR). Equation (3) simply states that the mass in each Lagrangian cell does not change with time.

Momentum is transferred from the photospheric radiation field to the wind through the radiative acceleration term. In our calculations, we use a phenomenological radiative acceleration term which has the form

$$g_{\rm rad} = g_{\rm max} f(T)(R_*/r)^2 , \quad (5)$$

where $g_{\rm max}$ is the maximum value of the radiative acceleration, and $f(T)$ is a function of the local wind temperature, T, but independent of the density. We adopt a form for $f(T)$ based on the model of MacGregor, Hartmann, and Raymond (1979) for stars with properties similar to τ Sco:

$$f(T) = \begin{cases} 1 & \text{if } T \leq 7.4 \times 10^4 \text{ K} \\ \exp(-T/T_0)/(3T/T_0) & \text{if } T > 7.4 \times 10^4 \text{ K} \end{cases},$$

where $T_0 = 2.8 \times 10^5$ K. At temperatures below 7.4×10^4 K, $g_{\rm rad}$ is independent of the wind temperature. At higher temperatures, the radiative acceleration decreases because of the decrease in the fractional abundances of ions most capable of absorbing the photospheric radiation. For example, in the high-temperature shock regions, C, N, and O can become fully ionized, and under these conditions would not contribute to the radiative force. The conditions near the base of the wind are not well-constrained by observations, so we simply select $g_{\rm max}$ so that material introduced at the base of the wind is accelerated to a higher velocity than the fluid in front of it, and that the maximum wind velocity is consistent with observations.

The energy conservation equation for the fluid is given by

$$\rho C_v \frac{\partial t}{\partial t} + \rho \left(\frac{\partial \epsilon}{\partial \rho}\right)_T \frac{\partial \rho}{\partial t} = \frac{1}{r^2}\frac{\partial}{\partial r}\left(r^2 \kappa_P \frac{\partial T}{\partial r}\right) + \frac{(P+Q)}{\rho}\frac{\partial \rho}{\partial t} - n n_e \Lambda , \quad (6)$$

where ϵ is the specific internal energy, C_v is the specific heat capacity and constant volume, κ_P is the plasma thermal conductivity, n is the nuclei number density, n_e is the electron density, and Λ is the plasma radiative cooling rate. The first term on the right-hand side represents energy transport by electron thermal conduction. This tends to be important only in the high-temperature regions of the shock since $\kappa_P \propto T^{5/2}$. On the other hand, radiative cooling tends to be important only at temperatures less than about 2 to 3 million degrees at wind densities relevant to τ Sco. For simplicity, we have used a steady-state ionization model in which collisional ionization is balanced with collisional, radiative, and dielectronic recombination (MacFarlane 1988). To account for heating by the photospheric radiation field, we restrict the wind temperature to be above 2.3×10^4 K.

Mass is added at the base of the wind at a constant rate. In practice, this is modeled by initially placing a large number of Lagrangian mass cells below the stellar "surface." As the calculation proceeds, mass flows from below the surface into the wind. Mass below the surface is assumed to be unaffected by the forces on the right-hand side of equation (4). As mass cells enter the wind, they are accelerated by the radiative force term. The total number of Lagrangian mass cells in our calculations was 172, of which 100 were initially below the surface of the star.

The entire wind above the photosphere feels the radiative acceleration given by equation (5). A fluid element that begins far above the photosphere in the calculation will not attain a velocity much greater than its initial velocity because $g_{\rm rad}$ decreases as $1/r^2$. Thus, as mass is injected into the wind from the surface of the star, it is accelerated to a higher velocity than the material ahead of it. This method of creating shocks is analogous to abruptly increasing the acceleration felt by the wind at $t = 0$. Eventually, a high-density shock region forms as the faster material supersonically overtakes the slower material.

The initial conditions in our calculations are as follows. The velocity distribution is given by

$$v(r) = 0.05 v_{\rm init} + 0.95 v_{\rm init}(1 - R_*/r) , \quad (7)$$

where $v_{\rm init}$ is an adjustable parameter. This form was chosen to avoid unphysical conditions at $r = R_*$. The density distribution was initialized using the steady-state mass flux relation $\rho = \dot{M}/4\pi r^2 v$. The wind was initially isothermal, with a temperature approximately equal to the stellar effective temperature. The calculations were run out to simulation times of roughly 15 hr so that the shocks could be followed out to distances of roughly 20 stellar radii.

In practice, $v_{\rm init}$, $\dot{M}$, and $g_{\rm max}$ were taken to be adjustable parameters with the following constraints. The quantity $\dot{M}$ was restricted to lie between the values of 0.7×10^{-8} $M_\odot$ yr^{-1} (LR) and 6.6×10^{-8} $M_\odot$ yr^{-1} (Gathier, Lamers, and Snow 1981). The value of $g_{\rm max}$ was varied to provide a terminal velocity consistent with the observed value ($\geq$2000 km s^{-1}; LR). Finally, we chose $v_{\rm init}$ to provide temperatures and velocity jumps at the shock fronts consistent with those deduced from X-ray observations.

IV. RESULTS

a) Shock Structure and Evolution

In this section, we present results from numerical calculations for an isolated shock region moving through a model wind for τ Sco. All of the results are from calculations using the following parameters: $\dot{M} = 1 \times 10^{-8}$ $M_\odot$ yr^{-1}, $g_{\rm max} = 1 \times 10^5$ cm s$^{-2} = 7.1 g_*$ (see eq. [5]), and $v_{\rm init} = 500$ km s^{-1} (see eq. [7]). The quantity $\dot{M}$ was adjusted to give an emission measure in the shock zone consistent with X-ray observations. Results for the shock structure are presented in Figure 1. The plots show the temperature, velocity, number density of nuclei, and pressure as a function of distance from the center of the star at times of 4.4, 9.3, and 14.6 hr. In effect, $t = 0$ can be thought of as the time at which the radiative acceleration increases and causes the shock to form. The dashed curve at $r > R_*$ in each plot represents the initial wind conditions. The vertical dashed curve at $r = R_*$ represents the stellar photosphere. The wind attains a velocity of 200 km s^{-1} at a radius of $r \simeq 1.9$ R_*, and a maximum velocity of roughly 2800 km s^{-1} far from the star. Since the maximum velocity inferred from UV observations probably occurs at a point close enough to the star that occultation effects are able to suppress the emission component of the P Cygni profiles, we feel the velocities

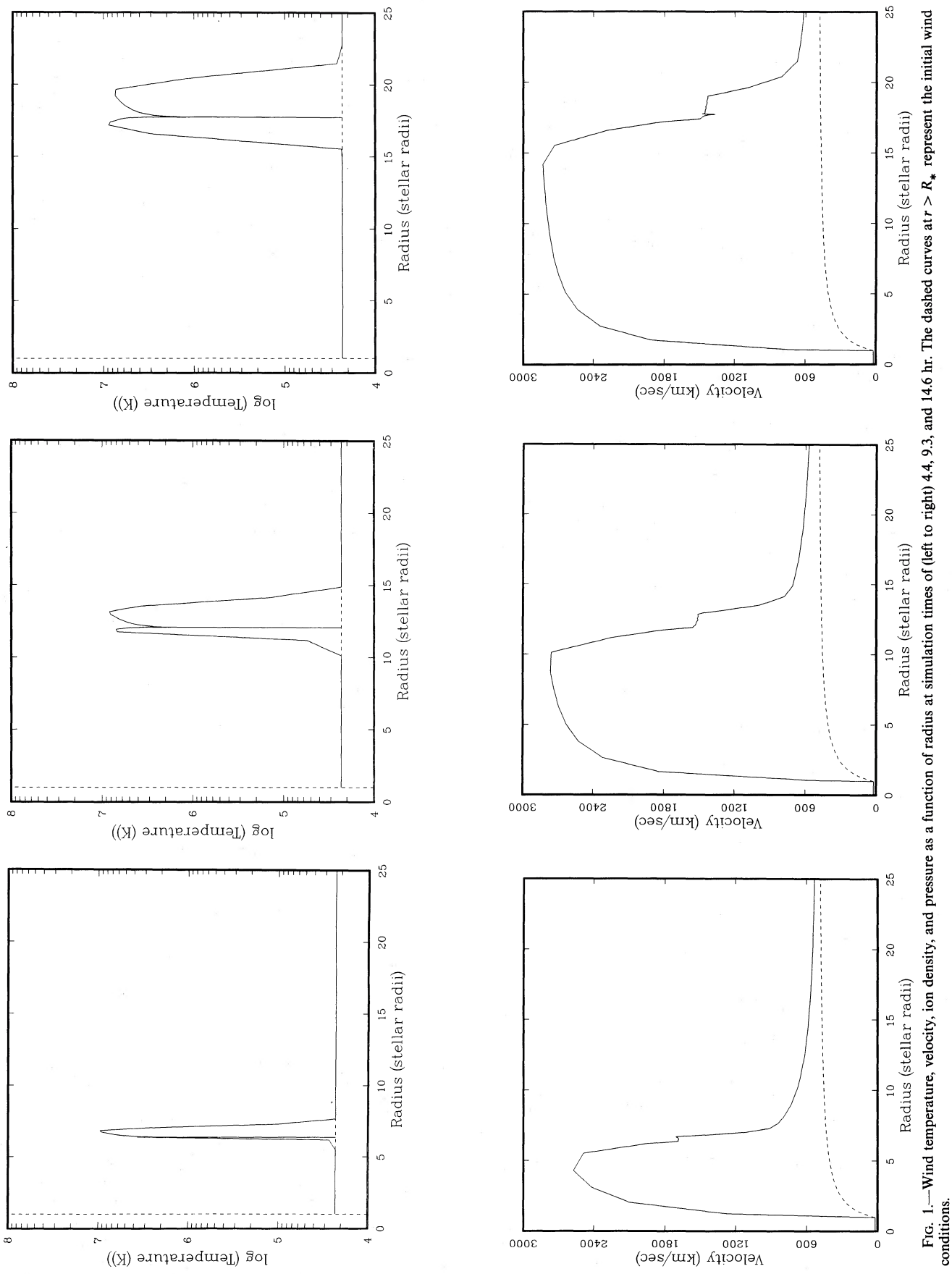

FIG. 1.—Wind temperature, velocity, ion density, and pressure as a function of radius at simulation times of (left to right) 4.4, 9.3, and 14.6 hr. The dashed curves at $r > R_*$ represent the initial wind conditions.

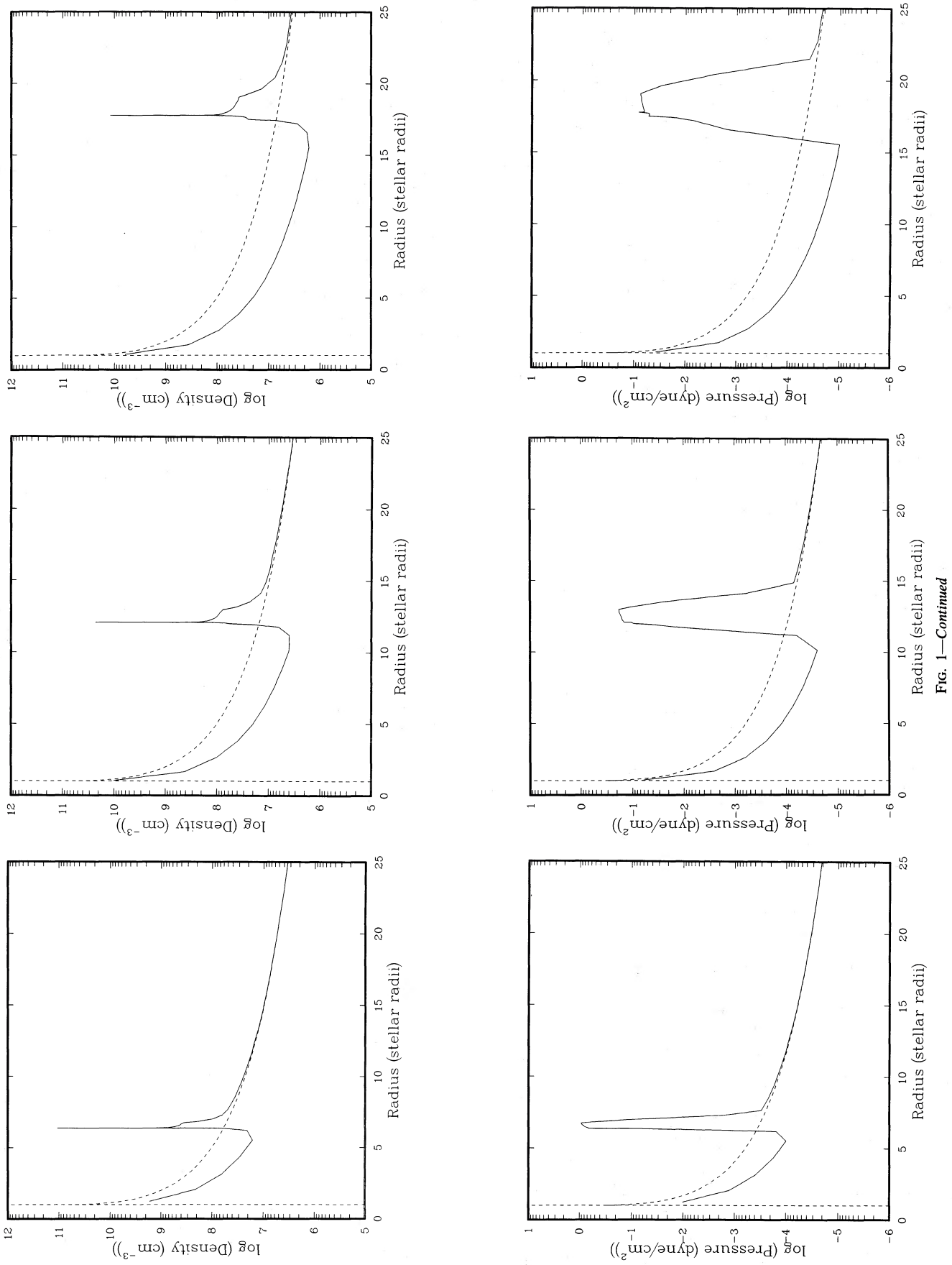

FIG. 1—*Continued*

shown in Figure 1 are reasonably consistent with observational data.

Soon after the calculation begins, a density discontinuity with a rather large density increase forms on the starward side of the compressed region as material near the star is accelerated by radiative pressure. This "driven wave" occurs because energy is continually pumped into the shock region from the starward side (see, e.g., Parker 1963). A shock front forms on the forward (outer) side of the compressed region as material is swept up by the shock. This is most easily seen in the temperature and pressure profiles. Another noticeable feature in Figure 1 is the formation of a "reverse" shock. This forms as a result of mass being added at the back of the compressed region. At later times, after a substantial amount of mass has been driven into the reverse shock, the "contact surface" (i.e., the region where the density attains its maximum value) is seen to lie near the center of the compressed region. The amount of mass in the contact region is $\sim 10^{23}$ g, which is typically distributed over 20 grid points. Unshocked material is racing supersonically toward the contact surface from both sides, creating the double shock region in which both the forward and reverse shocks propagate away from the contact surface. This situation is similar to that described by Hundhausen and Gentry (1969) in regards to the solar wind.

The temperatures in the shock heated wind range from 10^6 K to 10^7 K. The temperature within the reverse shock region is seen to increase with time, as does the velocity jump across the reverse shock increases. In Figure 1, the wind velocity within the compressed region remains roughly constant with time while the wind velocity of the unshocked wind on the starward side of the reverse shock, and hence the relative fluid velocity, increases. The temperature within the contact region remains rather cool due to radiative cooling effects. When the density in the contact region drops sufficiently ($r_{\rm shock} \gtrsim 20\ R_*$), the temperature in the contact region rises because the energy is conducted into the contact region faster than it can escape radiatively. We have also performed calculations in which energy transport by thermal conduction is neglected. In this case temperatures can be much higher behind the shock fronts. We find conduction limits the temperatures in our calculations to a maximum of about 2×10^7 K. For this reason, temperatures are significantly lower than predicted by equation (2). We conclude that conduction effects are important in the extended atmospheres of stars for which temperatures of $\gtrsim 10^7$ K are inferred from X-ray observations.

Within the shock region, the pressure and fluid velocity are roughly constant, with the velocity being about 1500 km s^{-1}. The density peaks at the contact surface and decreases outward toward each shock front. A sharp density gradient forms at each shock front with a density jump of $n_s/n_0 = 4$ ($n_0 \equiv$ density of unshocked fluid). Starward of the inward facing shock, the density increases as r decreases. The shocks in Figure 1 are seen to have finite widths; i.e., the change in conditions at each shock front are not discontinuous. This is caused by artificial viscosity spreading each shock over several mesh points.

The fact that large velocity jumps exist at both the forward and reverse shock fronts in our calculations raises the interesting possibility that this type of forward/reverse shock pair could be responsible for the characteristic two-temperature X-ray spectra observed for many hot stars. On the other hand, these spectra could likely also be produced by multiple shock regions in which only one of the forward/reverse shock pair was very strong, such as those described by OCR. Both models have strong reverse shocks capable of heating material to several million degrees, and high-density, nearly constant velocity regions which can qualitatively account for the narrow absorption features observed in P Cygni profiles of stars with denser winds. Thus shock models are able to account for a variety of features observed at both UV and X-ray wavelengths.

The velocity profiles in Figure 1 show that the shocked material is decelerating as it moves outward. This raises questions concerning Rayleigh-Taylor instabilities of the dense shell. The reverse shock is stable because the material is decelerating. A test element with enhanced density that is slightly displaced in the starward direction would not be displaced farther by deceleration. However, the forward shock appears to be unstable. Although we have not carried out a detailed analysis of the instability, we can estimate the rate of growth in the unstable regions. The deceleration of the region is seen to be roughly $a = 10^2$ cm s^{-2}. Thus, the maximum velocity of a displaced fluid element relative to its surroundings is at and its corresponding displacement is $d = gt^2/2$. For time scales ~ 10 hr, $d/R_* \simeq 0.1$. Thus Rayleigh-Taylor instabilities may lead to some mixing of the unshocked wind with dense material near the forward shock. However, the X-ray emission from the bulk of the shocked material will not be significantly affected by instabilities.

b) X-Ray Spectra

As the shock region propagates away from the star, the X-ray emission decreases as the density in the region drops due to expansion. The time-dependence of the X-ray emission measure in our hydrodynamic calculations is shown in Figure 2. This curve represents the contribution from material with temperatures above 10^6 K. The mass of material with temperatures between 10^5 and 10^6 K is small because of rapid radiative cooling effects. The dashed line at $EM = 3 \times 10^{54}$ cm^{-3} represents the observed X-ray emission measure (Swank 1985). Unfortunately, τ Sco was observed only once with the *Einstein* SSS. Because of this, we can only attempt to reproduce

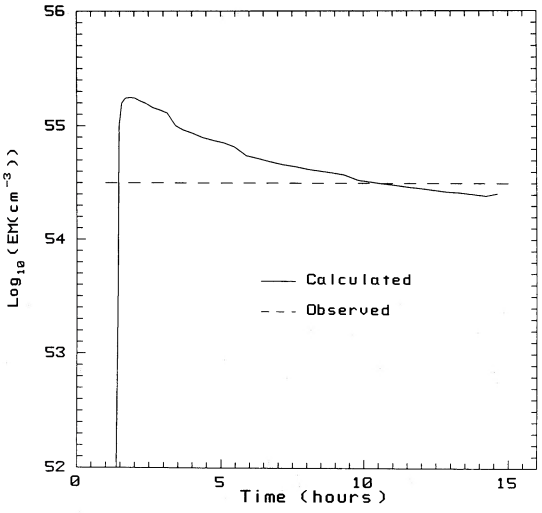

FIG. 2.—X-ray emission measure of shocked material with $T > 10^6$ K. The dashed curve represents the observed emission measure.

this single "time-averaged" spectrum. At times prior to 1.4 hr, which corresponds to a shock radius of 2.5 R_*, none of the wind has been shock-heated to temperatures above 10^6 K. This is simply an artifact of the manner in which we allow the shocks to form. Calculations performed to study the growth of shocks due to radiatively driven instabilities in isothermal winds find that strong shock can begin to form near 1.5 R_* (OCR).

At times ~ 2 hr, the calculated X-ray emission measure exceeds the SSS value by roughly a factor of 5. The emission measure then decreases as the shock travels radially outward and lies with a factor of 2 of the SSS value during the period from 6 to 15 hr. The emission measure decreases roughly inversely with time and shock radius for the following reason. The mean density in the shock region falls as t^{-2} due to expansion. However, the mass of material that is heated by the forward and reverse shocks increases roughly $\propto t$. Since the X-ray emission measure is proportional to the density times the mass of hot material, it decreases as t^{-1}.

The rate at which shocks form in the winds of O and B stars is an open question. It is unclear whether there is any systematic variation in their X-ray emission spectra. Although not directly concerned with τ Sco, there is some observational evidence that the variability of narrow absorption features of O stars is correlated with rotation period (Henrichs, Kaper, and Zwarthoed 1988). This could be consistent with models in which strong shocks form every few dozen hours. In addition, Gry *et al.* (1984) and Snow, Wegner, and Kunasz (1980) have found evidence for variations in the mass-loss rates of several early-type stars over time scales of several hours, including the main sequence B star α Vir. They suggest that density enhanced "puffs" or "shells" of matter are ejected by these stars. Gry *et al.* suggest that these fluctuations may be driven by pulsational instabilities similar to those in β Cep stars.

Using the temperature distributions shown in Figure 1, we have computed the X-ray emission spectra from the shock region at 4.4, 9.3, and 14.6 hr. To do this, we used a recent version of the code developed by Raymond and Smith (1977) and assumed no reabsorption of radiation. Figure 3 shows the results from our shock model (*solid curves*) along with the spectrum deduced from *Einstein* SSS observations (*dashed curves*; $T_1 = 5.3 \times 10^6$ K, $EM_1 = 3 \times 10^{54}$ cm^{-3} and $T_2 = 1.5 \times 10^7$ K, $EM_2 = 3 \times 10^{53}$ cm^{-3}). We assumed a distance to τ Sco of 236 parsecs (Shull and Van Steenberg 1985).

In general, the calculated spectra are in quite good agreement with the observed spectrum. The calculated spectra are somewhat softer because of the absence of material with temperatures above 10^7 K. At 4.4 hr, the flux near 0.4 keV is a factor of a few higher than observed, while the flux from higher energy X-rays ($\gtrsim 1$ keV) lies closer to the observed values. At later times, the softer X-ray flux agrees well with the observed flux, while the higher energy flux is somewhat lower than observed. The relative contribution to the X-ray emission from material at different temperatures is shown in Figure 4, where the differential emission measure is plotted for the temperature distribution at 9.3 hr. It is seen that material with temperatures between 1×10^6 and 9×10^6 K contributes to the X-ray spectrum, with a somewhat larger contribution coming from the lower temperature material. We feel our results show that the observed X-ray spectrum from τ Sco can be reproduced quite well with a model in which portions of its wind are shock-heated to several million degrees, and that the X-ray emission from B stars is likely generated by shocks forming their winds.

c) *Consequences of a "Warm" Wind*

If the wind of τ Sco is warm, as suggested by LR and Hamann (1981), a heat source would be required to keep it warm as it expands. This can be seen by examining the cooling of the plasma as it adiabatically expands. According to LR, the material at the 250 km s^{-1} level of the wind is characterized by an electron temperature of 2.0×10^5 K, and the material at the 1000 km s^{-1} level by 1.6×10^5 K. Using the velocity law suggested by LR, expansive cooling of the wind should cause the electron temperature to decrease as

$$T \propto n_e^{2/3} \propto [(1 - w)^2/w]^{2/3},$$

where $w = v/v_\infty$ is the scaled velocity. The temperatures should therefore drop by a factor of at least 5 as a wind parcel is accelerated from 250 km s^{-1} to 1000 km s^{-1}, far greater than the 25% inferred from UV observations. If radiative cooling rate is greater than the expansive cooling rate in the unshocked wind, the temperature drop would be even greater. Thus, if the LR interpretation of UV data is correct, a heating mechanism is required to keep the wind temperature high as it expands.

The EUV emission spectrum of τ Sco would differ dramatically from that predicted by our shock model if the material near the base of its wind was warm. This is shown in Figure 5, where the EUV spectrum computed for our shock model (*solid curve*) is compared with the spectrum for a warm wind (*dashed curve*). The warm wind spectrum assumes an isothermal wind with an emission measure of 10^{56} cm^{-3}. The warm wind flux is considerably larger at wavelengths above 100 Å, but drops rapidly at shorter wavelengths. In the shock model spectrum, a number of Fe lines are present at $\lambda \sim 70$–120 Å. Future observations at EUV wavelengths, such as those envisioned with the *EUVE* satellite, should provide valuable data for determining the properties of B star winds (Cassinelli *et al.* 1989).

V. CONCLUSIONS

We have shown that strong shocks propagating through the wind of the B0 V star τ Sco may indeed be the source of its X-ray luminosity. Results from our hydrodynamic calculations indicate that the observed X-ray spectrum for τ Sco can be approximately reproduced by a shock model using a mass-loss rate and wind velocity consistent with UV observations. As the shock region moves away from the star in our calculations, a second "reverse" shock forms at the back of the compressed region as a result of material being supersonically driven into the slower fluid ahead of it. Between the forward and reverse shocks lies a high-density contact region, which remains relatively cold due to radiative cooling effects. Our calculations raise the prospect that the characteristic two-temperature X-ray spectrum observed for many OB stars may be caused by the formation of double shock regions in their winds.

The evidence for the presence of shocks in the winds of hot stars is now quite strong. Analysis of X-ray spectral observations (Cassinelli *et al.* 1981) indicates that the X-ray source in several O stars is embedded far out into their winds. In addition, our calculations show shock structures with velocity plateaus which qualitatively account for the narrow absorption features observed in the P Cygni profiles of many stars. The observed difference between the terminal velocities and the velocities of the narrow absorption components is consistent with the magnitude of the fluid velocity discontinuities at the shock fronts in our calculations.

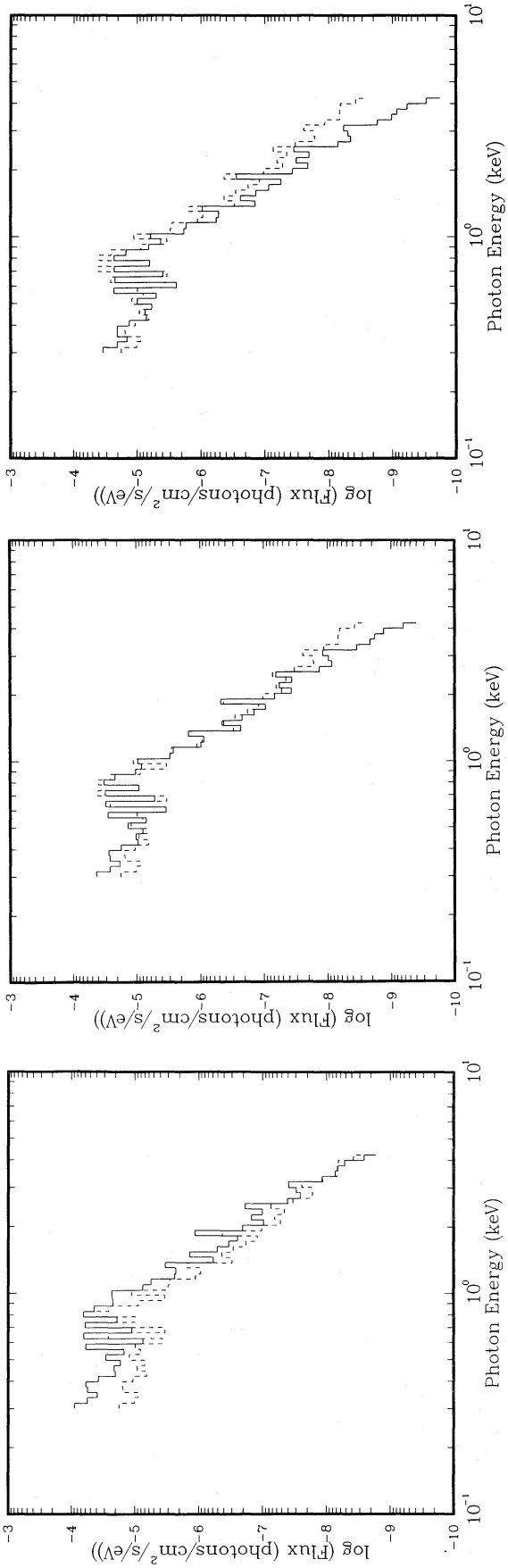

FIG. 3.—X-ray emission spectra for the shock structures shown in Fig. 1. The simulation times are (from left to right) 4.4, 9.3, and 14.6 hr. The dashed curves represent the spectrum deduced from *Einstein* SSS observations.

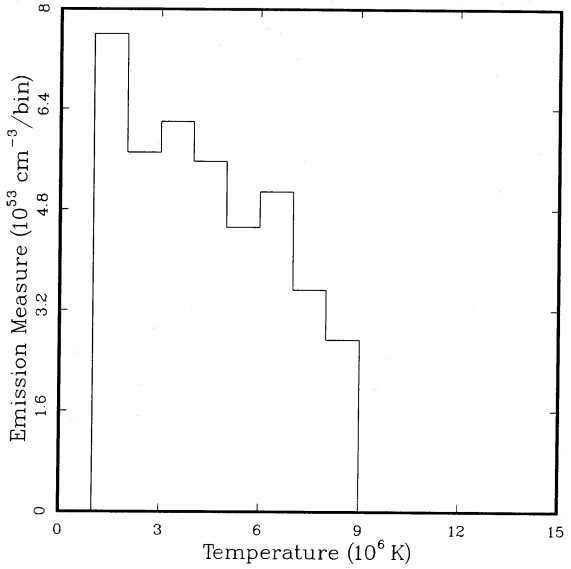

FIG. 4

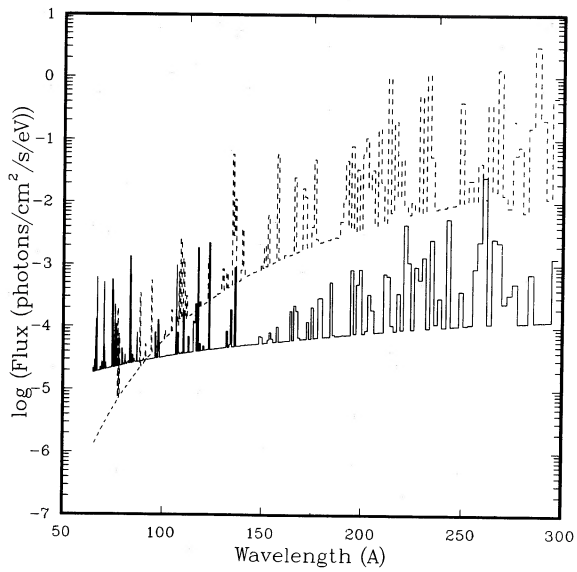

FIG. 5

FIG. 4.—Calculated differential emission measure at 9.3 hr

FIG. 5.—EUV emission spectrum from the shock region at 9.3 hr (*solid curve*). EUV spectrum computed for a "warm" wind (*dashed curve*).

The existence of strong shocks in the winds of early-type stars could be observationally confirmed by high-resolution X-ray or EUV measurements. At a temperature of 5×10^6 K, oxygen is essentially fully ionized, with approximately 3×10^{-3} of it in the form of hydrogen-like O VIII (Jordan 1969). If the X-ray source is moving at a velocity of 3000 km s^{-1} with respect to the star, the transition frequencies of O VIII should be shifted by ~ 0.2 Å (or $\sim 1\%$) for the Lyα transition near 19 Å, thereby spreading the line over an interval of 0.4 Å for a spherically expanding wind. In addition, emission lines for a variety of Fe ions should be present in the EUV portion of the spectrum around 70–250 Å (Cassinelli *et al.* 1989). Because the next generation of orbiting observatories will provide line strength information, they will be able to discriminate among the current models for superionization and X-ray emission.

J. J. M. has been supported in part by a grant from Lawrence Livermore National Laboratory. J. P. C. was supported by NASA grant NAG8-602. We wish to thank John Raymond and Stan Owocki for useful comments on this paper, and Henny Lamers for discussions concerning the properties of τ Sco. Computing support has been provided by the National Science Foundation through the San Diego Supercomputer Center.

REFERENCES

Cassinelli, J. P. 1985, in *The Origin of Nonthermal Heating/Momentum in Hot Stars*, ed. A. B. Underhill and A. G. Michalitsionos (NASA Publ. 2358), p. 2.
———. 1986, in *Instabilities in Luminous Early-Type Stars*, ed. H. J. G. L. M. Lamers and C. W. H. de Loore (Dordrecht: Reidel), p. 273.
Cassinelli, J. P., MacFarlane, J. J., Welsh, B., Vallerga, J., and Veddar, P. 1989, to appear in *Extreme Ultraviolet Astronomy*, ed. R. F. Malina.
Cassinelli, J. P., and Olson, G. L. 1979, *Ap. J.*, **229**, 304.
Cassinelli, J. P., and Swank, J. H. 1983, *Ap. J.*, **271**, 681.
Cassinelli, J. P., Waldron, W. L., Sanders, W. T., Harnden, F. R., Rosner, R., and Vaiana, G. S. 1981, *Ap. J.*, **250**, 677.
Castor, J. I., Abbott, D. C., and Klein, R. I. 1975, *Ap. J.*, **195**, 157 (CAK).
Collura, A., Sciortino, S., Serio, S., Vaiana, G. S., Harnden, F. R., and Rosner, R. 1989, *Ap. J.*, **338**, 296.
Gathier, R., Lamers, H. J. G. L. M., and Snow, T. P. 1981, *Ap. J.*, **247**, 173.
Gry, C., Lamers, H. J. G. L. M., and Vidal-Madjar, A. 1984, *Astr. Ap.*, **137**, 29.
Hamann, W. R. 1981, *Astr. Ap.*, **100**, 169.
Henrichs, H. F. 1988, in *O, Of, and Wolf-Rayet Stars*, ed. P. Conti and A. Underhill (NASA SP-497), p. 199.
Henrichs, H. F., Kaper, L., and Zwarthoed, G. A. A. 1988, in *A Decade of UV Astronomy with the IUE Satellite* (ESA SP-281, Vol. **2**), p. 145.
Hundhausen, A. J. 1985, in *Collisionless Shocks in the Heliosphere: A Tutorial Review*, ed. R. G. Stone and B. T. Tsurutani (AGU Geophysical Monograph 34), p. 37.
Hundhausen, A. J., and Gentry, R. A. 1969, *J. Geophys. Res.*, **74**, 6229.
Jordan, C. 1969, *M.N.R.A.S.*, **142**, 501.
Krolic, J. H., and Raymond, J. C. 1985, *Ap. J.*, **298**, 660.
Lamers, H. J. G. L. M., Gathier, R., and Snow, T. P. 1982, *Ap. J.*, **258**, 186.
Lamers, H. J. G. L. M., and Morton, D. 1976, *Ap. J. Suppl.*, **32**, 715.
Lamers, H. J. G. L. M., and Rogerson, J. B. 1978, *Astr. Ap.*, **66**, 417 (LR).
Long, K. S., and White, R. L. 1980, *Ap. J. (Letters)*, **239**, L65.
Lucy, L. B. 1982, *Ap. J.*, **255**, 286.
Lucy, L. B., and White, R. L. 1980, *Ap. J.*, **241**, 300.
MacFarlane, J. J. 1988, *Comput. Phys. Commun.*, submitted.
MacGregor, K. B., Hartmann, L., and Raymond, J. C. 1979, *Ap. J.*, **231**, 514.
Morton, D. C. 1979, *M.N.R.A.S.*, **189**, 57.
Mullan, D. J. 1984, *Ap. J.*, **283**, 303.
Olson, G. L., and Castor, J. I. 1981, *Ap. J.*, **244**, 179.
Owocki, S. P., and Rybicki, G. B. 1984, *Ap. J.*, **284**, 337.
Owocki, S. P., Castor, J. I., and Rybicki, G. B. 1988, *Ap. J.*, **235**, 914 (OCR).
Parker, E. N. 1963, *Interplanetary Dynamical Processes* (New York: Wiley).
Pauldroch, A. 1987, *Astr. Ap.*, **183**, 295.
Peterson, R. R., MacFarlane, J. J., and Moses, G. A. 1988, University of Wisconsin Fusion Technology Institute Report UWFDM-660.
Prinja, R. K., and Howarth, I. D. 1986, *Ap. J. Suppl.*, **61**, 357.
Raymond, J. C., and Smith, B. W. 1977, *Ap. J. Suppl.*, **35**, 419.
Rogerson, J. B., and Upson, W. L. 1977, *Ap. J. Suppl.*, **35**, 37.
Rybicki, G. B., Owocki, S. P., and Castor, J. I. 1988, *Ap. J.*, submitted.
Shull, J. M., and Van Steenberg, M. 1985, *Ap. J.*, **294**, 599.
Snow, T. P., Wegner, G. A., and Kunasz, P. B. 1980, *Ap. J.*, **238**, 643.
Swank, J. H. 1985, in *The Origin of Nonthermal Heating/Momentum in Hot Stars*, ed. A. B. Underhill and A. G. Michalitsionos (NASA Publ. 2358), p. 86.
Von Neumann, J., and Richtmyer, R. 1950, *J. Appl. Phys.*, **21**, 232.
Waldron, W. 1984, *Ap. J.*, **282**, 256.
———. 1989, personal communication.
Zeldovich, Y. B., and Raizer, Y. P. 1966, *Physics of Shock Waves and High-Temperature Hydrodynamic Phenomena* (New York: Academic).

JOSEPH P. CASSINELLI: Department of Astronomy, University of Wisconsin, Washburn Observatory, Madison, WI 53706

JOSEPH J. MACFARLANE: Fusion Technology Institute, University of Wisconsin, 1500 Johnson Drive, Madison, WI 53706